Image-set based Classification using Multiple Pseudo-whitened Mutual Subspace Method

Osamu Yamaguchi[1,2] and Kazuhiro Fukui[1]
[1]Department of Computer Science, Graduate School of Systems and Information Engineering, University of Tsukuba, Japan
[2]Corporate Research and Development Center, Toshiba Corporation, Japan

Keywords: Image-set based Classification, Whitening Transformation, Multiple Pseudo-Whitened Mutual Subspace Method, Ensemble Method, CNN Features.

Abstract: This paper proposes a new image-set-based classification method, called Multiple Pseudo-Whitened Mutual Subspace Method (MPWMSM), constructed under multiple pseudo-whitening. Further, it proposes to combine this method with Convolutional Neural Network (CNN) features to perform higher discriminative performance. MPWMSM is a type of subspace representation-based method like the mutual subspace method (MSM). In these methods, an image set is compactly represented by a subspace in high dimensional vector space, and the similarity between two image sets is calculated by using the canonical angles between two corresponding class subspaces. The key idea of MPWMSM is twofold. The first is to conduct multiple different whitening transformations of class subspaces in parallel as a natural extension of the whitened mutual subspace method (WMSM). The second is to discard a part of a sum space of class subspaces in forming the whitening transformation to increase the classification ability and the robustness against noise. We demonstrate the effectiveness of our method on tasks of 3D object classification using multi-view images and hand-gesture recognition and further verify the validity of the combination with CNN features through the Youtube Face dataset (YTF) recognition experiment.

1 INTRODUCTION

For the past few decades, many image set-based techniques have been proposed (Zhao et al., 2019). These techniques have been applied to face recognition (Taskiran et al., 2020), 3D object recognition (Wang et al., 2018a), and gesture recognition (Wang et al., 2018b), and are an essential technology in computer vision.

In this paper, we propose a new image-set-based classification, called Multiple Pseudo-Whitened Mutual Subspace Method (MPWMSM), which is constructed under multiple pseudo-whitening transformations. MPWMSM is a type of subspace representation-based method like the mutual subspace method (MSM) (Maeda and Watanabe, 1985; Yamaguchi et al., 1998) . In subspace-based methods, image set is compactly represented as a subspace, features are extracted by projection from the subspace representation to a discriminative space, and classification is performed using the angle between the subspaces as a similarity. In order to improve the discriminative performance, the Constrained Mutual Subspace Method (CMSM) (Fukui and Yamaguchi, 2003), the Multiple Constraint Mutual Subspace Method (MCMSM) (Nishiyama et al., 2005), and the Whitened Mutual Subspace Method (WMSM) (Kawahara et al., 2007) have been proposed as methods to perform feature extraction before the mutual subspace method.

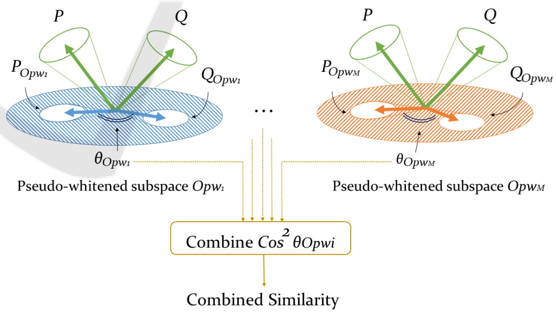

Figure 1: Overview of proposed Multiple Pseudo-Whitened Mutual Subspace Method.

Fig. 1 shows the overview of the proposed MP-WMSM. As the discriminant space in the proposed method, we adapt the whitening transformation with

Yamaguchi, O. and Fukui, K.
Image-set based Classification using Multiple Pseudo-whitened Mutual Subspace Method.
DOI: 10.5220/0010836500003122
In *Proceedings of the 11th International Conference on Pattern Recognition Applications and Methods (ICPRAM 2022)*, pages 296-306
ISBN: 978-989-758-549-4; ISSN: 2184-4313

a modified eigenvalue weighting, which is called the pseudo-whitening transformation (O_{pw_i} in Fig. 1). The components of whitening transformation with larger index are heavily weighted by the scaling factors that are highly sensitive to noise in the training data. In practice, disturbances due to noise can be observed and the classification using these components causes performance degradation. Discarding a part of a sum space of class subspaces in forming the whitening transformation increases the classification ability and the robustness against noise. Next, the two subspaces, P and Q, to be compared are transformed by multiple projection calculation using O_{pw_i} independently as shown in Fig. 1. Each projection O_{pw_i} can be used with a transformation consisting of a subset of the training data. Lastly, the similarity between the transformed subspaces is calculated respectively, and the final similarity is obtained by integrating multiple similarities. The combination of multiple feature extractions can achieve even higher accuracy due to the effect of ensemble learning with reducing overtraining and small variances.

Furthermore, in recent years, Convolutional Neural Network (CNN) features have shown high effectiveness in discriminative performance in various fields (Razavian et al., 2014; Azizpour et al., 2016). Several works have been already published showing the performance improvement by combining the mutual subspace method with CNN features (Sogi et al., 2018; Sakai et al., 2019). In our study, we use off-the-shelf CNN features without retraining Deep Convolutional Neural Networks (DCNNs) to reduce the training cost for the target domain. While we could take advantage of the training data to improve the CNN features with further fine-tuning, it is necessary to first ensure that the subspace-based feature extraction for image set works well.

The contributions of this paper include the following:

- To improve the noise tolerance to the whitening transformation, we classified the discriminative subspace into three categories based on the analysis of the eigenspectrum and studied the pseudo-whitening transformation.
- The MPWMSM method, which combines multiple feature extraction based on ensemble learning, is used to improve performance using subspace representations of off-the-shelf CNN features without retraining DCNNs.
- We applied the proposed method to several applications and confirmed its effectiveness. As a result, we achieved the state-of-the-arts accuracy for YouTube Faces dataset (YTF) using the latest deep learning features.

The paper is organized as follows. First, we outline the conventional algorithms of MSM, CMSM, and WMSM in section 2. In order to propose a new discriminant space, we review each method in terms of how it introduces the discriminant space. Section 3 describes an extension of Whitening transformation by modification of eigenvalue weighting and an integrated similarity calculation of multiple feature extraction methods similar to ensemble learning. In section 4, we compare the performance on 3D object recognition, gesture recognition, and video-based face recognition using a dataset for image-set based recognition. Finally we conclude our paper by summarizing the paper.

2 RELATED WORK ON SUBSPACE-BASED METHODS

In this section, we describe the subspace-based matching algorithms (Yamaguchi et al., 1998) and constrained mutual subspace method (Fukui and Yamaguchi, 2003) and the whitened mutual subspace method (Kawahara et al., 2007). Finally, we describe the problem of WMSM and analyze it from the view of eigenspectrum. Then, we make a comparison of the transformation in CMSM and WMSM.

2.1 Mutual Subspace Method

Mutual Subspace Method (MSM) (Maeda and Watanabe, 1985) is a method that approximates the entire pattern variation by a subspace and measures the similarity by the angle between the subspaces. This is an extension of the Subspace Method (Oja, 1983), which performs identification based on the minimum angle θ_1 between two subspaces, the input subspace and the reference subspace.

The identification based on this minimum angle uses the concept of a canonical angle and is generalized by multiple canonical angles. Between the m-dimensional subspace P and the n-dimensional subspace Q, n canonical angles ($n < m$) can be defined, and the first canonical angle θ_1 is the minimum angle between the two subspaces.

The second canonical angle θ_2 is the minimum angle measured in the direction orthogonal to the minimum canonical angle θ_1. Similarly, the following n canonical angles $\theta_i (i = 1 \dots n)$ can be obtained sequentially. The minimum canonical angle is determined by the angle between the two subspaces, θ_1, in the equation (1). Similarity S between patterns is then used for classification (Yamaguchi et al., 1998).

$$S = \cos^2\theta_1 \tag{1}$$

The $\cos^2\theta_1$ is the maximum eigenvalue λ_{max} of the following matrix $\mathbf{X}$.

$$\mathbf{X}\mathbf{a} = \lambda\mathbf{a} \tag{2}$$

$$\mathbf{X} = (x_{mn}) \quad (m,n = 1\ldots N_d) \tag{3}$$

$$x_{mn} = \sum_{l=1}^{N}(\psi_m,\phi_l)(\phi_l,\psi_n) \tag{4}$$

where ψ_m,ϕ_l are the m,lth orthonormal basis vectors in the subspaces P and Q, where (ψ_m,ϕ_l) is the inner product of ψ_m and ϕ_l, and N_d is the number of basis vectors in the subspace.

The canonical angles between the two subspaces can be obtained plurals as described. In practice, we consider the value of the mean of the canonical angles,

$$S[t] = \frac{1}{t}\sum_{i=1}^{t} cos^2\theta_i, \tag{5}$$

as the similarity between two subspaces. The value $S[t]$ reflects the structural similarity between two subspaces.

2.2 Constrained Mutual Subspace Method and Generalized Differential Subspace

In the previous section, we explained how MSM classifies a set of feature vectors in the original vector space. However, the original space is not exactly favorable for discriminating the subspaces, and it is desirable to embed each subspace in a more discriminative space.

To improve the discrimination performance, the input subspace P and the reference subspace Q are projected onto the constrained subspace C consisting of the components effective for discrimination, and the canonical angles are measured for the projections P_c and Q_c, as shown in Figure 2. This method adds the projection onto the constrained subspace to the mutual subspace method and is called Constrained Mutual Subspace Method (CMSM) (Fukui and Yamaguchi, 2003).

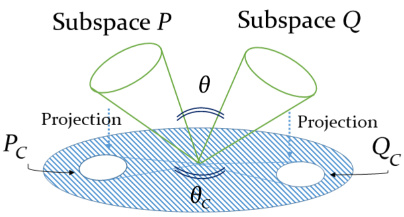

Figure 2: Concept of CMSM.

Futhermore, there is also a method that uses the generalized differential subspace (Fukui and Maki, 2015). The generalized difference subspace D is obtained by first calculating the sum matrix $G = \sum_{i=1}^{k}\mathbf{P}_i$, where $\mathbf{P}_i$ are the projection matrices of R n-dimensional reference subspaces. The basis vectors are then obtained by performing the following eigenvalue decomposition:

$$Gd = \lambda d \tag{6}$$

where the eigenvectors $\mathbf{d_i}$ correspond to the i-th eigenvalue λ_i in descending order. Finally, only the N_B eigenvectors with smallest eigenvalue are kept as the basis vectors for D. Such dimension is set experimentally.

As shown in Fig. 3, the generalized difference subspace D is obtained by removing the principal component space M, which doesn't contain useful information for discrimination, from the sum space of all class subspaces. Geometrically, by removing the space M, the angle between each class subspace projected to the generalized difference subspace is expanded.

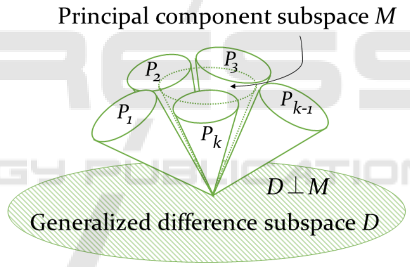

Figure 3: Concept of generalized difference subspace.

2.3 Whitened Mutual Subspace Method

This section describes the whitening transformation of a set of subspaces as a process to emphasize the differences between the subspaces representing each class. The whitening transformation for a set of subspaces is formulated as an approximate solution to the minimum value problem of the objective function, which becomes smaller as the angle between the subspaces increases. Let the set of d-dimensional subspaces of each class be $V_1,\ldots,V_R$ and the d canonical angles of V_i and V_j be $\theta_{ij}^{(1)},\ldots,\theta_{ij}^{(d)}$. Then, the following equation holds for the sum of the squares of the cosines of the canonical angles.

$$\sum_{1\leq<i\leq R}\sum_{k=1}^{d} cos^2\theta_{ij}^{(k)} = C_1\sigma^2 + C_2, \tag{7}$$

where C_1, C_2 are positive constants and σ^2 is the variance of the eigenvalues of the autocorrelation matrix G of the set of subspaces defined below:

$$G = \frac{1}{R}\sum_{i=1}^{R}\mathbf{P_i}. \tag{8}$$

$\mathbf{P_i}$ is a projection matrix $(1 \leq i \leq R)$ defined in the basis $\psi_{i1}, \ldots, \psi_{iN_p}$ of V_i as following equation,

$$\mathbf{P_i} = \sum_{k=1}^{N_p}\psi_{ik}\psi_{ik}^T. \tag{9}$$

From this equation, we can see that the smaller the variance of the eigenvalues of the matrix G, the wider is the angle between the subspaces that generated G. Therefore, the variance of the eigenvalues of the autocorrelation matrix G is minimized by the whitening transformation W, which sets all eigenvalues to 1, as defined below.

$$G = B\Lambda B^T. \tag{10}$$

$$W = \Lambda^{-1/2}B^T, \tag{11}$$

where Λ is the diagonal matrix of the eigenvalues of the autocorrelation matrix G, and B is the matrix of its eigenvectors arranged vertically.

Figure 4 shows how the whitening transformation expands the angles between the subspaces. Since the whitening transformation spreads the angles uniformly, the pairs of subspaces with smaller angles between them will expand more. Therefore, when the whitening transformation is applied to the subspace of a certain class, the angle expands in the subspace of similar classes, emphasizing the difference.

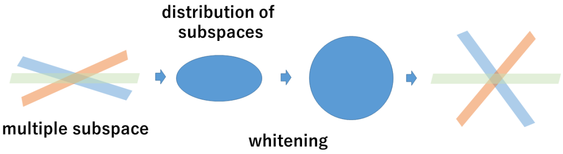

Figure 4: The ellipse and the circle in the center of the figure represent the distribution of subspaces. Whitening makes the distribution uniform.

2.4 The Problems of Previous Methods

2.4.1 Analysis in View of the Eigenspectrum

In order to prevent the reference subspaces of each class from being similar to each other, the whitened mutual subspace method linearly transforms the reference subspaces into a feature space where the angles between the reference subspaces are apart, thereby improving the discrimination accuracy.

However, we have observed in the literature (Fukui and Yamaguchi, 2006) an interesting result for the ETH-80 dataset (Leibe and Schiele, 2003).

Table 1: Results for 3D object recognition in (Fukui and Yamaguchi, 2006).

	Accuracy (%)			
	S[1]	S[2]	S[3]	S[4]
MSM	72.7	73.7	76.3	74.3
CMSM-215	75.7	81.3	76.3	73.7
CMSM-200	73.3	81.0	79.3	77.7
CMSM-190	71.0	73.0	73.0	75.7
WMSM(OMSM)	51.3	54.0	56.0	54.0

As we can see in Table. 1, despite the whitening transformation, WMSM perform worse than MSM. This means that feature extraction has lost its meaning despite the use of discriminant transformations with the subspace. To improve this performance degradation, we revise the feature extraction by whitening transformation.

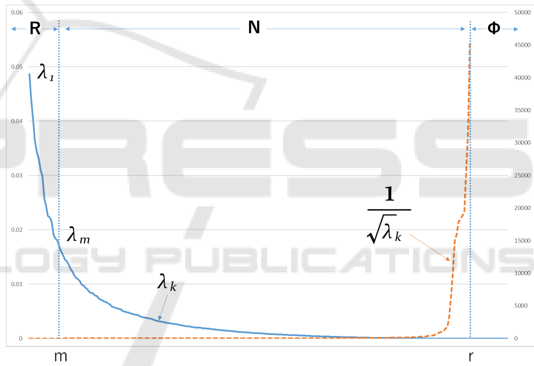

Figure 5: A real distribution of eigenvalues in descending order (solid line) and the weights of whitening transformation (dashed line). m denotes split point between Reliable subspace (R) and Noise subspace (N). r denotes split point between Noise subspace and Null subspace(Φ).

Fig. 5 shows the distribution of eigenvalues of G (Eq. (6)) in descending order and the weights $(1/\sqrt{\lambda_k})$ of whitening transformation. The components of whitening transformation of larger index are heavily weighted by the scaling factors.

The discussion of the eigenspectrum has been discussed in (Jiang et al., 2008). This paper points out that noise turbulence and poor estimates of small eigenvalues due to the finite number of training samples are the culprits. Due to the limited number of training samples, the eigenvalues for a dimension can be so small that they do not represent the true variance of that dimension well. This may result in severe problems if their inverses are used as the weight for the whitening transformation.

We estimate the eigenspectrum using the equation in (Jiang et al., 2008). The two parameters α and β, and the estimating equation are defined by Eq. (12). (13) and (14).

$$\alpha = \frac{\lambda_1 \lambda_m (m-1)}{\lambda_1 - \lambda_m}, \tag{12}$$

$$\beta = \frac{m\lambda_m - \lambda_1}{\lambda_1 - \lambda_m}, \tag{13}$$

$$\hat{\lambda}_k = \frac{\alpha}{k+\beta}, \tag{14}$$

where λ_1 is the maximum eigenvalue, λ_m is the eigenvalue of the split points m, and $\hat{\lambda}_k$ is the estimated eigenvalue. The subspaces are divided into three categories, i.e., Reliable subspace (R), Noise subspace (N), and Null subspace (ϕ) (Jiang et al., 2008). The split point indicates the index m that separates the reliable subspace (R) from the noise subspace (N), as shown in Fig. 5.

We introduce the eigenvalue ratios to observe how much they differ from the estimated variance,

$$\frac{\hat{\lambda}_{k+1}}{\hat{\lambda}_k} = \frac{\alpha}{k+1+\beta} \times \frac{k+\beta}{\alpha} = \frac{k+\beta}{k+1+\beta}. \tag{15}$$

Eq. (15) is a monotonically decreasing function and it calculates the ratio between $\hat{\lambda}_k$ and $\hat{\lambda}_{k+1}$.

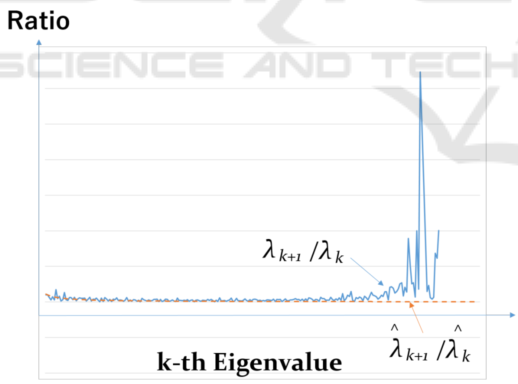

Figure 6: The comparison of the real eigenvalue ratio (solid line) and estimated eigenvalue ratio (dashed line) . The oscillations arises in the components with large index.

Figure 6 plots the real and estimated eigenvalue ratio values. It is desirable that the eigenvalue ratios always decay, even in the high-dimensional part of the whitening transformation. However, in the large index eigenvalue part, many of them deviate from the estimated values. This disturbance leads to large oscillations in the inverse eigenspectrum. The components with large index k are strongly sensitive to noise due to training data, leading to poor recognition performance on test data.

In the next section, the discussion will focus on controlling the magnitude of the eigenvalues of the autocorrelation matrix of the basis vectors used to compute the feature extraction.

2.4.2 Comparison between Projection to Constrained Subspaces and Whitening Transformation

The constrained mutual subspace method (CMSM) and the whitened mutual subspace method (WMSM) are both methods to obtain the transformation matrix based on the autocorrelation matrix G of the projection matrix generated from the reference subspace. The projection matrix $\mathbf{P}_i$ is defined by Eq. (16), where ψ_{ij} is the j-th orthonormal basis vector of the reference subspace of the i-th category and N_p is the number of basis vectors of the reference subspace.

In the CMSM, the constrained subspace $\mathbf{O}_{CMSM}$ is defined using the projection matrix of each category by Eq. (18).

$$\mathbf{P}_i = \sum_{j=1}^{N_p} \psi_{ij}\psi_{ij}^T, \tag{16}$$

$$\mathbf{G} = \frac{1}{R}(\mathbf{P}_1 + \mathbf{P}_2 + \cdots + \mathbf{P}_R), \tag{17}$$

$$\mathbf{O}_{CMSM} = \sum_{k=1}^{N_B} \phi_k \phi_k^T, \tag{18}$$

where R is the number of reference subspaces, ϕ_k is the kth eigenvector selected from the smaller eigenvalues of the matrix G, and N_B is the number of eigenvectors of the matrix G.

On the other hand, in the whitening mutual subspace method, the transformation matrix for whitening the reference subspaces $\mathbf{O}_{WMSM}$ is defined by the Eq. (19).

$$\mathbf{O}_{WMSM} = \mathbf{\Lambda}^{-\frac{1}{2}}\mathbf{B}^T. \tag{19}$$

As before, $\mathbf{B}$ is the matrix of eigenvectors of $\mathbf{G}$, and $\mathbf{\Lambda}$ represents the diagonal matrix of the eigenvalues of $\mathbf{G}$. $\mathbf{O}_{CMSM}$ is represented using the following $\mathbf{C}_p$.

$$\mathbf{O}_{CMSM} = \mathbf{C}_p\mathbf{B}^T, \tag{20}$$

$$\mathbf{C}_p = diag(0,0,0,\ldots,0,1,1,1,1). \tag{21}$$

In this case, C_p is the diagonal matrix of rank N_B. This weight distribution is shown in Figure 7. The graph shows the weights of the eigenvectors in each method. In CMSM, only the vectors after a particular dimension are used, and the weight is 1.0 in each case. In the WMSM, on the other hand, the weights

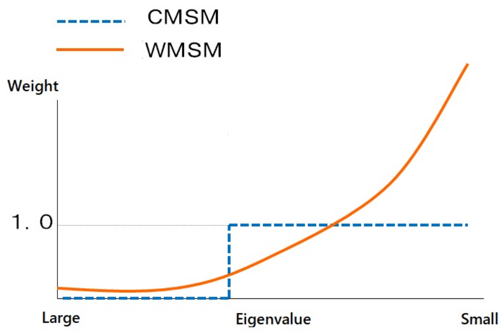

Figure 7: Weighting of Constraint subspace and Whitening transformation.

are the square root of the reciprocals of the eigenvalues, and thus the weights become larger for higher dimensions. This figure also shows that eigenvectors of lower dimensions, which are discarded in CMSM, are given small values in WMSM, while eigenvectors of higher dimensions are given large weights. In the WMSM, the components extracted by the high-dimensional eigenvectors are given more importance, which may cause cases of high similarity between classes and may lead to a decrease in performance. This does not occur in the CMSM due to introducing constant weights.

3 PROPOSED METHOD

In this section, we describe our method, MPWMSM. We introduce the pseudo-whitening transformation. After that, we describe the proposed method which combines multiple feature extraction.

3.1 Introduction of Pseudo-whitening Transformation

As in the case of the CMSM, we propose to select the features to be extracted by setting the weights of some basis vector components to zero, which is like a combination of WMSM and CMSM.

Figure 8 shows the weighting of the whitening transformation with different parts set to zero. In Fig. 8(a), the high-dimensional part is set to 0, and in Fig. 8(b), the low-dimensional part is set to 0. Furthermore, in Fig. 8(c), both parts are set to 0 simultaneously.

Such weighting has been already discussed in terms of eigenspectrum regularization models (ERMs) (Jiang et al., 2008; Tan et al., 2018). These methods focus on weighting using the full rank. The CMSM is considered to be divided into two sub-

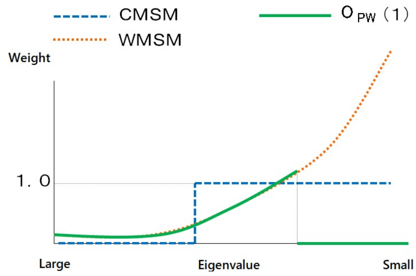

(a) Eliminate high-dimensional parts

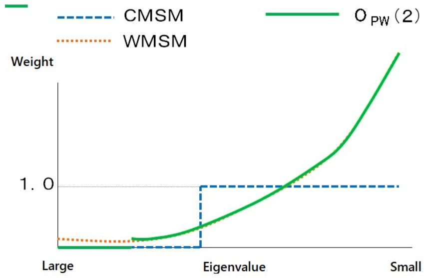

(b) Eliminate low-dimensional parts

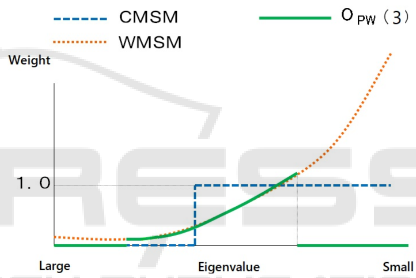

(c) Eliminate both parts of high and low-dimension

Figure 8: Variation of changing weights of whitening transformations.

spaces, principal component subspace and generalized difference subspace as shown in Figure 3, and the split points are defined for the binary weights shown in Figure 7. In our method, we divide the subspace into three categorized subspaces: principal component subspace, reliable difference subspace, and noise subspace, as shown in Figure 9. The discriminative space is defined by their combination.

To achieve this, we filter some of the diagonal components of the matrix $\mathbf{\Lambda}$, such as some of the small eigenvalues or some of the large eigenvalues, setting them to 0, and make changes to it as a pseudo-whitening matrix $\mathbf{O}_{PW}$.

Then, by replacing the whitening matrix $\mathbf{O}_{WMSM}$ of the whitening mutual subspace method with the pseudo-whitening matrix $\mathbf{O}_{PW}$, it is expected to improve the results for the cases where the WMSM does not outperform MSM.

The pseudo-whitening matrix $\mathbf{O}_{PW}$ is defined by

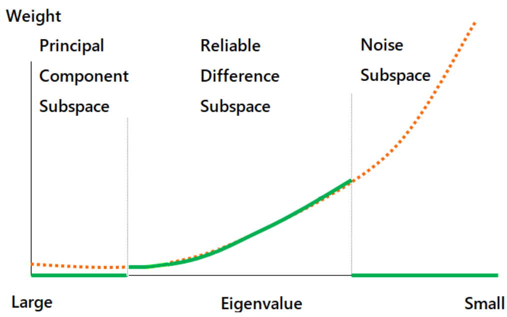

Figure 9: Subspaces divided into three categorized parts in our method. As for the weights of Principal Component Subspace and Noise Subspace, we control them by setting them to zero.

the Equation (22).

$$\mathbf{O}_{PW} = \mathbf{C}_s \mathbf{\Lambda}^{-\frac{1}{2}} \mathbf{B}_P{}^T = \mathbf{\Lambda}_s{}^{-\frac{1}{2}} \mathbf{B}^T. \tag{22}$$

Here, $\mathbf{B}$ is a matrix of eigenvectors, $\mathbf{\Lambda}$ is a diagonal matrix of eigenvalues, and $\mathbf{C}_s$ is a diagonal matrix with 0 and 1 elements given by the equation (23). $\mathbf{\Lambda}_s^{-\frac{1}{2}}$ is given by the equation (24), where j and k denote the dimensions that define the range to be set to 0. Several of the eigenvalues of $\mathbf{\Lambda}$ are replaced by zeros. We can replace some eigenvalues with 0 using various $\mathbf{C}_s$.

$$\mathbf{C}_s = \begin{cases} diag(1,\dots,\underset{k}{1},\dots,1,0,\dots,0) \ \dots \ (a) \\ diag(0,\dots,0,\underset{j}{1},\dots,1,\dots,1) \ \dots \ (b) \\ diag(0,\dots,0,\underset{j}{1},\dots,\underset{k}{1},0,\dots,0) \ \dots \ (c) \end{cases} \tag{23}$$

$$\mathbf{\Lambda}_s^{-\frac{1}{2}} = \begin{cases} diag(\frac{1}{\sqrt{\lambda_1}},\frac{1}{\sqrt{\lambda_2}},\dots,\frac{1}{\sqrt{\lambda_k}},0,\dots,0) \ \dots \ (a) \\ diag(0,\dots,0,\frac{1}{\sqrt{\lambda_j}},\frac{1}{\sqrt{\lambda_{j+1}}},\dots,\frac{1}{\sqrt{\lambda_d}}) \ \dots \ (b) \\ diag(0,\dots,0,\frac{1}{\sqrt{\lambda_j}},\frac{1}{\sqrt{\lambda_{j+1}}},\dots,\frac{1}{\sqrt{\lambda_k}},0,\dots,0) \ \dots \ (c) \end{cases} \tag{24}$$

Therefore, the Mutual Subspace Method using the pseudo-whitening transformation $\mathbf{O}_{PW}$ is denoted as the Pseudo-Whitened Mutual Subspace Method (PWMSM).

3.2 Multiple Pseudo-whitened Mutual Subspace Method

This section presents the Multiple Whitened Mutual Subspace Method (MWMSM) and the Multiple Pseudo-Whitened Mutual Subspace Method (MPWMSM) in which we applied ensemble learning to the Whitened Mutual Subspace Method. This approach follows (Nishiyama et al., 2005)

To extract effective features for set-based image recognition, we transform the input subspace and the reference subspace into multiple feature transformation. In the experiment we obtained high performance compared with projecting onto a single transformation. To generate multiple transformations, we apply the framework provided by ensemble learning.

Figure 1 in Section 1 shows process diagram of Multiple Pseudo-Whitened Mutual Subspace Method (MPWMSM). The multiple pseudo-whitening transformations are represented by the projection matrix in Eq. (22).

To generate multiple feature extractor in this paper, we use the concept of Bagging (Breiman, 1996), which is based on an ensemble learning algorithm. Multiple classifiers are constructed using random sampling in Bagging. To apply this framework to generating feature extractor, we randomly select L' $(< L)$ subspaces from L class subspaces. Each projection subspace is generated independently using selected training subspaces.

In summary, we generate M constraint subspaces by the following steps:

1. Select L' class subspaces randomly without replacement.
2. Generate a projection subspace using selected L' class subspaces in Eq. (22).
3. Until M projection subspaces are generated, go to step 1.

To combine similarities obtained on each projection subspace, we define the combined similarity S_T as follows:

$$S_T = \sum_{i=1}^{M} \alpha_i S_{O_{pw_i}}, \tag{25}$$

where M is the number of the pseudo-whitening transformations; α_i is the i-th coefficient of O_{pw_i}; $S_{O_{pw_i}}$ is the similarity between $P_{O_{pw_i}}$ and $Q_{O_{pw_i}}$ projected onto O_{pw_i}.

4 EXPERIMENTS

In this section, we will present the experimental evaluation of our proposed method. We performed mainly three experiments, to be explained in the following subsections.

4.1 3D Object Recognition (ETH-80)

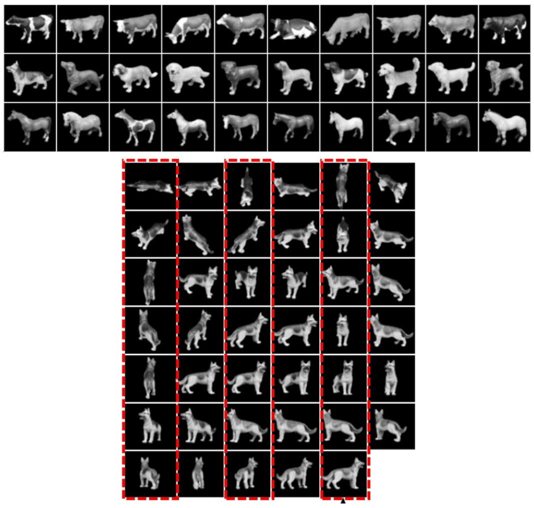

Figure 10: Object Recognition experiment using ETH-80. **Top:** Selected 30 classes for similar shape classification test. **Bottom:** All patterns of dog1 (the dotted columns are the training images).

We carried out our experiments using the ETH-80 dataset, which consists of 3D models taken from multiple viewpoints, as shown in Fig. 10. From this database, 30 models with similar shapes are extracted. The experimental conditions for these models are in accordance with the literature (Fukui and Yamaguchi, 2007). Therefore, CNN features are not used in this experiment for comparison with conventional protocols.

For each model, a set of images is taken from 41 viewpoints for each object, as shown in Figure 10. The viewpoints are the same for all models. Of these, the odd-numbered images (21) are used as the class subspace, while the even-numbered images (20) are used as the evaluation data. In other words, the learning perspective is different from the evaluation perspective. For the evaluation data, we took 10 images from i to i + 9 out of the 20 images to make one data set, and prepared a total of 10 evaluation sets by changing the starting frame i from 1 to 10. Therefore, the total number of trials is 300 (=10×30).

The original image was converted to a monochrome image of 16 × 16 pixels for the evaluation. Thus, the dimensionality of the data is 256. The dimensionality of the input subspace and the reference subspace of each class was set to 7, and the dimensionality of the subspace used for training (N_p) was set to 20. For direct comparison with WMSM, no multiplication is applied, and the evaluation is performed as $M = 1$ and $\alpha_1 = 1.0$ in Eq. (25).

Here, PWMSM (j, k) represents the case where the j-th to k-th elements in Eq. (23) are set to 1. Therefore, PWMSM(1, 256) is the same as WMSM.

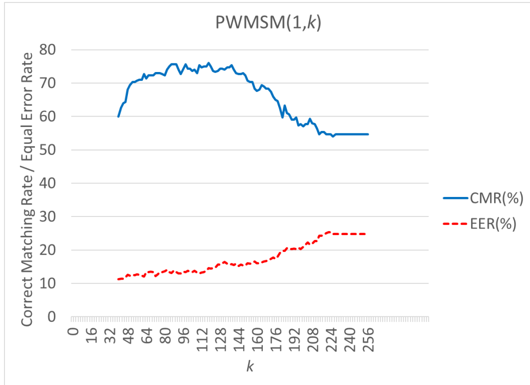

Figure 11: The correct matching rate and the equal error rate of PWMSM(1, k) for different dimension of k. O_{PW} is eliminated part of higher dimension.

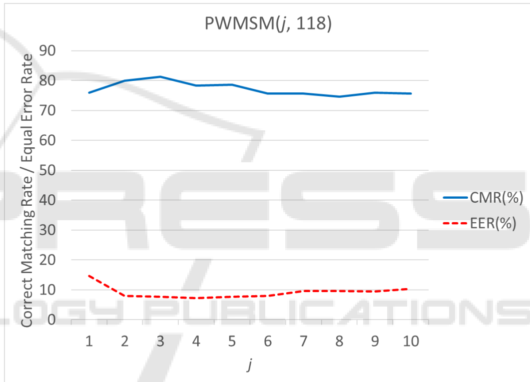

Figure 12: The correct matching rate and the equal error rate of PWMSM(j, 118) for different dimension of j. O_{PW} is eliminated both part of higher and lower dimension.

Figure 11 shows the correct matching rate and the equal error rate of PWMSM(1, k) for different dimension of k. The results were obtained by varying from the 40th dimension to the 256th dimension sequentially. This refers to classification accuracy improved to 76.0% compared to 54.6% for the original whitening transformation.

The result of fixing the 118th dimension at the maximum value and changing the elements of C_s of Eq. (23) from the low-dimensional part to 0, i.e. PWMSM(j, 118) is shown in Fig. 12. In this case, the results further improved to 81.4%. When compared to S[1] in Table 2, it is found to exceed the performance of other linear feature extraction schemes.

Our best performance of PWMSM was achieved when using 3 - 100 dimensions, resulting in 83.3% in classification accuracy. This is the best performance among the subspace-based methods we compared.

Table 2: Results for 3D object recognition.

	Acc. (%) by S[1]
MSM CMSM-215	72.7 75.7
WMSM	54.6
PWMSM (1, 118) PWMSM (3, 118) PWMSM (3, 100)	76.0 81.4 **83.3**
MWMSM MPWMSM (3, 104)	11.0 **84.0**

Table 2 summarizes the results and compares the proposed method with the results from a conventional linear feature extraction system.

In addition, feature selection performed by the PWMSM can embed the data in a smaller dimension than the original data dimension. We believe this is of great practical significance, as it improves the storage efficiency of the reference subspace and reduces computational cost.

Furthermore, to perform the multiple version of proposed methods, the MWMSM and MPWMSM, the training data is divided into three parts, and the discriminant transformation is created from 10 samples of each part. We confirmed that the performance could be further improved by the multiple pseudo-whitening transformations, while it gets worse by the multiple whitening transformations.

4.1.1 Hand Gesture Recognition (IPN Hand)

Hand gesture recognition (HGR) is an essential function of human-computer interaction, which has a wide range of applications. IPN Hand (Benitez-Garcia et al., 2021) is a video dataset for real-time hand gesture recognition. The gestures in this dataset focused on interaction with touchless screens, including 13 categories. In the 50 subjects, there are 16 females and 34 males. The dataset was collected from about 30 diverse scenes, with real-world variation in background and illumination.

We tried the Isolated HGR task, which is evaluated as the conventional classification metric. The data split the data by subject into training (74%) and testing (26%) sets, resulting in 148 training and 52 testing videos. The numbers of gesture instances in training and testing splits are 3,117 and 1,101, respectively. In this experiment, we use the RGB-seg used in literature (Benitez-Garcia et al., 2021). Semantic segmentation masks were provided as annotated data and we segmented the RGB images using the masks. The images are processed by the public pre-trained ResNet-100 model by ImageNet train, and 2048 dimensional features are extracted from the C5 layer. Note that the training data was not used to train the DCNNs. We use the training data only for subspace-based feature extraction.

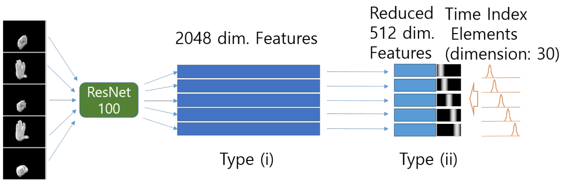

Figure 13: Frame Features for HGR. Type (i) is a 2048 dimensional feature extracted from DCNNs for each frame; Type (ii) uses features reduced to 512 dimensions from the original DCNNs features by PCA and add a time index element to represent the time transition.

Each gesture instance's start and end frame index in the video was manually labeled, providing enough information to train for forming the subspace. The video sequences are segmented into isolated gesture samples based on the beginning and ending frames manually annotated. We use classification accuracy to evaluate our method, which is the percent of correctly labeled examples.

Table 3 shows the results for IPN Hand classification. We tried two types of features as shown in Fig. 13. Type (i) is a 2048 dimensional feature extracted from DCNNs for each frame; Type (ii) uses features reduced to 512 dimensions from the original DCNNs features by PCA. Moreover, we add a 30-dimensional time index element to represent the time transition. For the time index, we let the normal distribution move along the time axis as shown in Fig. 13. They are equally divided according to the time length of each gesture and assigned to different locations of the peaks of the 30-dimensional indices.

Table 3: Results for IPN Hand. (i) 2048 dim. DCNNs Feature, (ii) Reduced 512 dim. DCNNs Feature with Time Index elements.

		Acc. (%)
(i)	MSM (S[1]) MSM (S[5]) WMSM (S[5]) PWMSM(S[5],(j, k)=(1, 388)) MPWMSM(S[5],(j, k)=(5, 388))	38.23 43.96 50.40 55.40 **57.00**
(ii)	MSM (S[10]) WMSM (S[10]) PWMSM (S[10],(j, k)=(20, 320)) MWMSM(S[10]) MPWMSM (S[10],(j, k)=(20, 400))	35.51 47.32 58.94 59.21 **60.13**
	3D versions of ResNet-50 (Benitez-Garcia et al., 2021)	75.11

The proposed method, MPWMSM, was found to be superior to these methods with other feature extraction. Although the performance is not as good as the 3D version of ResNet-50 tested in (Benitez-Garcia et al., 2021), it was confirmed that the subspace-based feature extraction is more effective for the original DCNN features.

4.1.2 Video-based Face Recognition (YTF)

Next, we experiment with recognition using video face image data. The YouTube Face dataset (YTF) is the most widely used benchmark for face recognition on video. It consists of 3,425 videos of 1,595 identities. In the YTF evaluation protocol, 5,000 video pairs are matched in 10 folds, and the average accuracy is required. Each fold consists of 500 video pairs, which are guaranteed to have mutually exclusive properties for the subject.

The current top accuracy for the YTF benchmark is SeqFace (Hu et al., 2018), which uses ResNet-64 based features to compute the final score by applying the simple average features of all faces in the video. In ArcFace (Deng et al., 2019), which uses ResNet-100 based feature trained by MS1Mv2 dataset (Deng et al., 2019). The simple average features are also applied to evaluate the results. Therefore, we apply the proposed method using state-of-the-art CNN features by deep learning.

As CNN features, we use the ResNet-100 model using ArcFace loss and trained on Glint360k dataset (An et al., 2021). We downloaded the public trained model published by InsightFace (InsightFace, 2021). The dimensionality of the feature vector is 512. For the YTF video data, five facial feature points are obtained using MTCNN (Zhang et al., 2016), and the face image is cropped to a size of 112x112 pixels. Note that fine-tuning using YTF data was not performed for DCNNs in this experiment.

Table 4: Results for YTF.

	Acc. (%)
Simple average features	98.22 ± 0.61
MSM (S[4])	98.28 ± 0.69
MWMSM (S[2])	98.30 ± 0.80
MPWMSM (S[2],(j, k)=(3, 277))	$\mathbf{98.38 \pm 0.60}$
SeqFace (Hu et al., 2018)	98.12
ArcFace (Deng et al., 2019)	98.02

We tried different parameters for the number of canonical angles (Eq. (5)), the number of dimensions of the reference subspace N_p (Eq. (16)), and the choice of weights (Eq. (23)). Table 4 shows evaluation results for YTF.

When comparing the results with those of Arcface (Deng et al., 2019), we can see that the accuracy is improved by using simple average features due to the increased training data (MS1Mv2 dataset to Glint360k dataset). Furthermore, the accuracy is improved by using MSM with the subspace representation of each video. S[4] shows that the best performance was obtained when the number of canonical angles of similarity was 4.

Since there are ten folds in YTF when testing a particular fold, we used one for testing and the remaining 9 folds to train the whitening transformation for MWMSM. Multiplication is then performed according to section 3.2.

In high-performance discriminative features, multiplication using WMSM was confirmed to be better than MSM. Note that random selection in bagging is not performed this time. Since there is no overlap of individual IDs in each fold, the whitening transformation/pseudo-whitening transformation is calculated using each fold's subspace. The dimensionality of the subspace used for training (N_p) was set to 20.

Finally, we can see that our proposed pseudo whitening transformation achieved the best results, with identification accuracy of 98.38%. The MPWMSM showed the same improvement over the MWMSM as confirmed by 4.1.1 and 4.1.2. We confirm that the proposed pseudo-whitening transformation is more effective than the whitening transformation.

5 CONCLUSION

This paper proposed the Multiple Pseudo-Whitened Mutual Subspace Method (MPWMSM), which performs multiple feature extraction by projecting the input and reference subspaces into multiple discriminative subspaces and then calculating and integrating multiple similarities. By selecting the weighting of the basis vectors of the whitening transformation, we confirmed the improvement of the accuracy by the pseudo-whitening transformation.

We demonstrated the effectiveness of our method on tasks of 3D object classification using multi-view images and hand-gesture recognition. We also verified the validity of the combination with CNN features through the YTF face recognition experiment. The experiment results show that our method can improve the performance in face recognition by extracting the features of the video without fine-tuning the DCNNs itself.

Future work includes automatic dimensionality setting of the pseudo-whitening space according to the data set.

REFERENCES

An, X., Zhu, X., Gao, Y., Xiao, Y., Zhao, Y., Feng, Z., Wu, L., Qin, B., Zhang, M., Zhang, D., and Fu, Y. (2021). Partial fc: Training 10 million identities on a single machine. In *Proceedings of the IEEE/CVF International Conference on Computer Vision (ICCV) Workshops*, pages 1445–1449.

Azizpour, H., Razavian, A. S., Sullivan, J., Maki, A., and Carlsson, S. (2016). Factors of transferability for a generic convnet representation. *IEEE Transactions on Pattern Analysis and Machine Intelligence*, 38(9):1790–1802.

Benitez-Garcia, G., Olivares Mercado, J., Sanchez-Perez, G., and Yanai, K. (2021). Ipn hand: A video dataset and benchmark for real-time continuous hand gesture recognition. *Proc. of IAPR International Conference on Pattern Recognition (ICPR)*, pages 4340–4347.

Breiman, L. (1996). Bagging predictors. *Machine Learning*, 24(2):123–140.

Deng, J., Guo, J., Xue, N., and Zafeiriou, S. (2019). Arcface: Additive angular margin loss for deep face recognition. *In IEEE/CVF Conference on Computer Vision and Pattern Recognition (CVPR)*, pages 4690–4699.

Fukui, K. and Maki, A. (2015). Difference subspace and its generalization for subspace-based methods. *IEEE Transactions on Pattern Analysis and Machine Intelligence*, 37(11):2164–2177.

Fukui, K. and Yamaguchi, O. (2003). Face recognition using multi-viewpoint patterns for robot vision. *11th International Symposium of Robotics Research (ISRR)*, pages 192–201.

Fukui, K. and Yamaguchi, O. (2006). Comparison between constrained mutual subspace method and orthogonal mutual subspace method. *Proc. of Subspace 2006*, pages 63–71. (In Japanese).

Fukui, K. and Yamaguchi, O. (2007). The kernel orthogonal mutual subspace method and its application to 3d object recognition. *Proc. of ACCV07*, pages 467–476.

Hu, W., Huang, Y., Zhang, F., Li, R., Li, W., and Yuan, G. (2018). Seqface: Make full use of sequence information for face recognition. *CoRR*, abs/1803.06524.

InsightFace (2021). Insightface model zoo. *GitHub repository*.

Jiang, X., Mandal, B., and Kot, A. (2008). Eigenfeature regularization and extraction in face recognition. *IEEE Transactions on Pattern Analysis and Machine Intelligence*, 30(3):383–394.

Kawahara, T., Nishiyama, M., Kozakaya, T., and Yamaguchi, O. (2007). Face recognition based on whitening transformation of distribution of subspaces. In *ACCV'07 Workshop Subspace 2007*.

Leibe, B. and Schiele, B. (2003). Analyzing appearance and contour based methods for object categorization. *Proc. of IEEE Conference on Computer Vision and Pattern Recognition*, pages 409–415.

Maeda, K. and Watanabe, S. (1985). A pattern matching mathod with local structure. *Trans. IEICE(D)*, J68-D(3):345–352. (In Japanese).

Nishiyama, M., Yamaguchi, O., and Fukui, K. (2005). Face recognition with the multiple constrained mutual subspace method. In *AVBPA*.

Oja, E. (1983). *Subspace Methods of Pattern Recognition*. Research Studies Press, England.

Razavian, A. S., Azizpour, H., Sullivan, J., and Carlsson, S. (2014). Cnn features off-the-shelf: an astounding baseline for recognition. *In IEEE Conference on Computer Vision and Pattern Recognition workshops*, pages 806–813.

Sakai, A., Sogi, N., and Fukui, K. (2019). Gait recognition based on constrained mutual subspace method with cnn features. In *2019 16th International Conference on Machine Vision Applications (MVA)*, pages 1–6.

Sogi, N., Nakayama, T., and Fukui, K. (2018). A method based on convex cone model for image-set classification with cnn features. *International Joint Conference on Neural Networks (IJCNN)*, pages 1–8.

Tan, H., Gao, Y., and Ma, Z. (2018). Regularized constraint subspace based method for image set classification. *Pattern Recognition*, 76:434–448.

Taskiran, M., Kahraman, N., and Erdem, C. E. (2020). Face recognition: Past, present and future (a review). *Digital Signal Processing*, 106:102809.

Wang, D., Wang, B., Zhao, S., Yao, H., and Liu, H. (2018a). Off-the-shelf cnn features for 3d object retrieval. *Multimedia Tools Appl.*, 77(15):1983319849.

Wang, T., Li, Y., Hu, J., Khan, A., Liu, L., Li, C., Hashmi, A., and Ran, M. (2018b). *A Survey on Vision-Based Hand Gesture Recognition: First International Conference, ICSM 2018, Toulon, France, August 2426, 2018, Revised Selected Papers*, pages 219–231. Springer.

Yamaguchi, O., Fukui, K., and Maeda, K. (1998). Face recognition using temporal image sequence. In *Proceedings of the 3rd. International Conference on Face and Gesture Recognition*.

Zhang, K., Zhang, Z., Li, Z., and Qiao, Y. (2016). Joint face detection and alignment using multitask cascaded convolutional networks. *IEEE Signal Processing Letters*, 23(10):1499–1503.

Zhao, Z.-Q., Xu, S.-T., Liu, D., Tian, W.-D., and Jiang, Z.-D. (2019). A review of image set classification. *Neurocomputing*, 335:251–260.